

Observation of strong coupling between one atom and a monolithic microresonator

Takao Aoki¹†, Barak Dayan¹, E. Wilcut¹, W. P. Bowen¹†, A. S. Parkins¹†, T. J. Kippenberg²†, K. J. Vahala² & H. J. Kimble¹

Over the past decade, strong interactions of light and matter at the single-photon level have enabled a wide set of scientific advances in quantum optics and quantum information science. This work has been performed principally within the setting of cavity quantum electrodynamics^{1–4} with diverse physical systems⁵, including single atoms in Fabry–Perot resonators^{1,6}, quantum dots coupled to micropillars and photonic bandgap cavities^{7,8} and Cooper pairs interacting with superconducting resonators^{9,10}. Experiments with single, localized atoms have been at the forefront of these advances^{11–15} with the use of optical resonators in high-finesse Fabry–Perot configurations¹⁶. As a result of the extreme technical challenges involved in further improving the multilayer dielectric mirror coatings¹⁷ of these resonators and in scaling to large numbers of devices, there has been increased interest in the development of alternative microcavity systems⁵. Here we show strong coupling between individual caesium atoms and the fields of a high-quality toroidal microresonator. From observations of transit events for single atoms falling through the resonator’s evanescent field, we determine the coherent coupling rate for interactions near the surface of the resonator. We develop a theoretical model to quantify our observations, demonstrating that strong coupling is achieved, with the rate of coherent coupling exceeding the dissipative rates of the atom and the cavity. Our work opens the way for investigations of optical processes with single atoms and photons in lithographically fabricated microresonators. Applications include the implementation of quantum networks^{18,19}, scalable quantum logic with photons²⁰, and quantum information processing on atom chips²¹.

The realization of large-scale quantum networks^{18,19} requires the capability to inter-connect many ‘quantum nodes’, each of which could consist of a microresonator containing a set of trapped atoms. The ‘quantum channels’ to connect these nodes would be optical fibres, with strong interactions in cavity quantum electrodynamics (QED) providing an efficient interface between light and matter. Here we provide a critical step towards a feasible quantum network by demonstrating strong coupling of single atoms to microresonators fabricated on silicon wafers in large numbers by standard lithographic techniques followed by a laser-reflow process²². Combined with the capability to couple light efficiently to and from such cavities directly via a tapered optical fibre²³, toroidal microcavities offer promising capabilities for new nonlinear interactions of single atoms and photons across distributed networks.

Our efforts follow the pioneering work of V. Braginsky *et al.*²⁴ and later studies²⁵ by employing the whispering-gallery modes of fused silica microtoroidal resonators²⁶. As shown in Fig. 1, a silicon chip containing a collection of 35 microtoroidal resonators is located

inside a vacuum chamber at 10^{-9} Torr and is positioned to couple a particular resonator to a tapered fibre. The toroids have major diameter $D \approx 44 \mu\text{m}$ and minor diameter $d \approx 6 \mu\text{m}$ (ref. 26). By judicious choice of the point of contact between the surface of the resonator and the tapered fibre, we attain critical coupling, in which the forward propagating power P_F in the fibre drops to near zero for the probe frequency ω_P equal to the cavity resonance frequency ω_C (ref. 23). Measurements of the cavity transmission in the absence of atoms are presented in Fig. 2. Note that the forward flux P_F and the associated transmission spectrum T_F are analogous to the reflected flux and reflection spectrum from a Fabry–Perot cavity²³. By varying the temperature of the silicon chip, the detuning $\Delta_{AC} \equiv \omega_C - \omega_A$ between ω_C and the atomic resonance at ω_A ($6S_{1/2}$; $F = 4 \rightarrow 6P_{3/2}$; $F' = 5'$ transition in caesium) can be controlled with an uncertainty of ± 2 MHz (Supplementary Information).

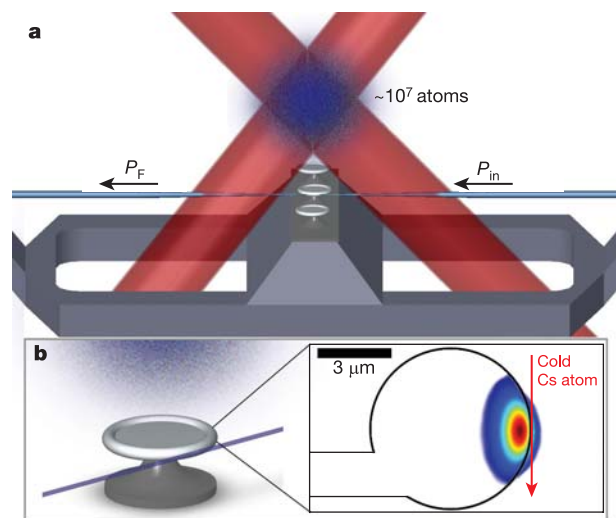


Figure 1 | Simple diagram of the experiment. **a**, A cloud of cold caesium atoms and the associated trapping lasers above an array of microtoroidal resonators. Light from the probe beam P_{in} is coupled into a resonator by way of the fibre taper, with the forward propagating output P_F coupled back into the taper from the resonator. **b**, Illustration of a SiO_2 microtoroidal resonator, fibre taper, and atom cloud. The calculated field distribution for the lowest-order resonator mode is shown by the colour contour plot on the right. Cold caesium atoms fall through the external evanescent field of this mode and are thereby strongly coupled to the resonator’s field.

¹Norman Bridge Laboratory of Physics 12-33, California Institute of Technology, Pasadena, California 91125, USA. ²T. J. Watson Laboratory of Applied Physics, California Institute of Technology, Pasadena, California 91125, USA. †Present addresses: Department of Applied Physics, The University of Tokyo, Tokyo 113-8656, Japan (T.A.); Physics Department, University of Otago, Dunedin 9016, New Zealand (W.P.B.); Department of Physics, University of Auckland, Auckland 1142, New Zealand (A.S.P.); Max Planck Institute of Quantum Optics, Garching 85748, Germany (T.J.K.).

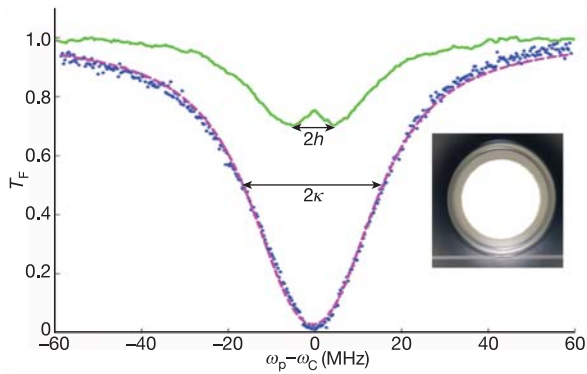


Figure 2 | Cavity transmission function $T_F = P_F/P_{in}$ as a function of probe frequency ω_p . The lower trace is taken for critical coupling, and the upper trace for conditions of under-coupling²³. From fits to such traces for critical coupling (red dashed curve), we find that $(\kappa, h)/2\pi = (17.9 \pm 2.8, 4.9 \pm 1.3)$ MHz, with κ, h being the overall cavity field decay rate and the scattering-induced coupling between the two counter-propagating modes of the microtoroid, respectively (see Supplementary Information for more details). Inset: photograph of a microtoroid and coupling fibre.

Cold atoms are delivered to the vicinity of the toroidal resonator from a small cloud of caesium atoms cooled to $T \approx 10 \mu\text{K}$ and located 10 mm above the silicon chip. Every 5 s, the cloud is dropped, resulting in about 2×10^6 atoms in a 3-mm ball at the height of the chip, with then a few dozen atoms passing through the external evanescent field of the toroidal resonator. By way of two single-photon detectors (D_{F1} , D_{F2}) (Supplementary Information), we continuously monitor the forward propagating signal P_F from a frequency-stabilized probe beam P_{in} coupled to the toroidal resonator. The interaction of an individual atom with the evanescent field destroys the condition of critical coupling, leading to an increase in

P_F . The measurement cycle then repeats itself for 2.5 s for a reference measurement, this time with no atomic cloud formed above the microtoroid.

Figure 3 displays typical records $C(t)$ for the number of single-photon detection events within time bins of $\delta t = 2 \mu\text{s}$ as functions of time t for the forward signal $P_F(t)$. Measurements are displayed with (Fig. 3a) and without (Fig. 3b) atoms for the case of equal probe and cavity frequencies, $\omega_p = \omega_c$, for $\Delta_{AC} \approx 0$, and with mean intracavity photon number $n_0 \approx 0.3$ for the forward circulating mode a of the toroidal resonator (Supplementary Information). The traces in both Fig. 3a and Fig. 3b exhibit background levels that result from the non-zero ratio $P_F/P_{in} \approx 0.005$ at critical coupling in the absence of atoms. However, Fig. 3a clearly shows sharp peaks of duration $\Delta t \approx 2 \mu\text{s}$ for the forward-propagating light $P_F(t)$, with an individual peak shown more clearly in the inset. Each event arises from the transit of a single atom through the resonant mode of the microtoroid, with about 30 events per cycle observed. Figure 3c examines the temporal profile of transit events in more detail by way of the cross-correlation $I(\tau)$ of photoelectric counts $C_1(t_1)$ and $C_2(t_1 + \tau)$ from the detectors D_{F1} and D_{F2} for P_F (Supplementary Information). This result agrees reasonably well with the theoretical prediction for atom transits through the calculated field distribution shown in Fig. 1b.

By applying a threshold requiring $C(t) \geq 6$ counts for $C(t)$ as in Fig. 3a, b, we find the average time dependence $\bar{C}_{\geq 6}(t)$ over about 100 measurement cycles. Figure 3d displays the results both with and without atoms, with the average counts $\sum_6(t)$ derived from $\bar{C}_{\geq 6}(t)$ by summing over successive time bins $\delta t = 2 \mu\text{s}$ for 1-ms intervals. The peak in transit events is consistent with the expected distribution of arrival times for atoms dropped from our atom cloud. By contrast, negligible excess events (that is, $C(t) \geq 6$) are recorded for the cases without atoms.

Focusing attention to the central region indicated by the dashed lines in Fig. 3d, we examine in Fig. 3e the probability $P(C)$ of recording C counts within $\delta t = 2 \mu\text{s}$. Evidently, when the atom

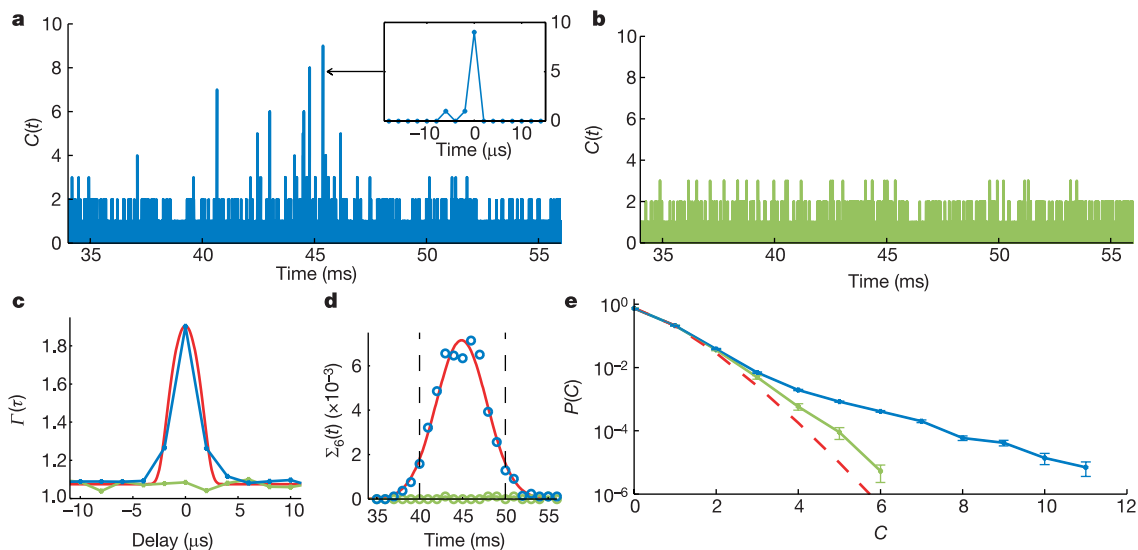


Figure 3 | Measurements of the forward signal P_F in the presence of falling atoms (blue) and without atoms (green). **a, b**, Single-photon counting events $C(t)$ as a function of time t after the release of the cold atom cloud at $t = 0$, with **(a)** and without **(b)** atoms dropped. $C(t)$ gives the total number of counts recorded for time bins of $\delta t = 2 \mu\text{s}$ duration. The inset in **a** shows the time profile for a single-atom transit. **c**, Normalized cross-correlation $I(\tau)$ of the forward signal counts from two detectors (D_{F1} , D_{F2}), showing the time profile associated with atom transit events. The smooth (red) curve is the theoretically predicted average cross-correlation for a transit event with one atom, taking into account the drop height of 10 mm and the spatial shape of the mode, as depicted in Fig. 1b. **d**, Counts $\sum_6(t)$ obtained from

$\bar{C}_{\geq 6}(t)$ by summing over 1-ms intervals, compared with a gaussian distribution that fits the rate of atom transits assuming a 3-mm (full-width at half-maximum) cloud of cold atoms dropped from 10 mm above the microtoroid. **e**, Probability $P(C)$ of detecting C counts within time bins of $\delta t = 2 \mu\text{s}$ for the central interval shown by the vertical dashed lines in **d**, compared with poissonian statistics (red) with the same mean number of counts (~ 0.25 per $2 \mu\text{s}$). The excess probability above the poissonian level in the no atoms case is predominantly due to instability in the cavity temperature, which results in small fluctuations in the forward flux. Error bars show ± 1 s.d.

cloud is present, there is a statistically significant increase (of at least 15σ) in the number of events with $C \geq 4$. These are precisely the events illustrated by the inset in Fig. 3a and the cross-correlation in Fig. 3c, and are associated with single-atom transits near the surface of the toroidal resonator. By varying the value of n_0 we have confirmed that the large transit events evident in Fig. 3 are markedly decreased for $n_0 \geq 1$ photons, which indicates the saturation of the atom–cavity system.

A quantitative description of our observations in Fig. 3 of individual atom transits requires the development of a new theoretical model in cavity QED. In the Supplementary Information we present such a model and show that the underlying description of the interaction of an atom with the fields of the toroidal resonator is in terms of normal modes (A,B) (Supplementary Fig. 1), which have mode functions $\psi_{A,B}(\rho, x, z)$ that are standing waves ($\cos kx$, $\sin kx$) around the circumference x of the toroid, with ρ the radial distance from the surface and z the vertical coordinate. Mode functions $\psi_{A,B}(\rho, x, z)$ have a calculated peak coherent coupling $g_0/2\pi$ of 70 MHz for the lowest-order modes of our resonator (such as that illustrated in Fig. 1b). The normal modes A,B result from the coupling of two oppositely directed travelling waves by scattering at rate h , with the resulting mode splitting seen in Fig. 2. Note that the presence of two normal modes leads to a $\sqrt{2}$ increase in the coupling constant in our case in contrast with that predicted by the Jaynes–Cummings model for an atom interacting with a single travelling-wave mode (see Supplementary Information for further details).

Guided by this theory, we have performed a series of measurements similar to those presented in Fig. 3 to determine the coherent coupling rate g_0 for interactions of single atoms with our toroidal resonator, but now with various values of the atom–cavity detuning Δ_{AC} , keeping the probe resonant with the cavity: $\omega_C \approx \omega_p = \omega_A + \Delta_{AC}$. The

qualitative idea is that large single-atom transit events will occur only over a range of detunings Δ_{AC} determined by g_0 . Specifically, the decrease in the forward transmission T_F induced by atom transits as a function of Δ_{AC} is described by a lorentzian with width β set by g_0 (Supplementary Information). In our case, $g_0 = g_0(\rho, x, z) \approx g_0(\rho, x, Vt)$, where V is the velocity of the dropped atoms in the z direction. Thus, a numerical integration was performed over ρ , x and t to derive the theoretical expectation for $T_F(\Delta_{AC})$, presented in Fig. 4a for three values of g_0^m , where g_0^m is the maximal coupling that an atom can experience in its interaction with the cavity modes. Indeed, we see that the width β grows monotonically with g_0^m . However, the average value of T_F is not readily measured in our current experiment, in which we expect many short individual transits, some of which are too weak to be distinguished from the background noise (see Fig. 3e). A parameter that describes our actual experimental measurements more closely is the probability of obtaining a transit that results in transmission above a certain threshold. The two measures are closely related, such that this probability decreases with detuning Δ_{AC} in the same fashion as T_F .

Figure 4b–d presents the results of our measurements for the average number of transit events per atom drop, $N_{\text{drop}}^{\text{av}}(C \geq C_0)$, which have photoelectric counts greater than or equal to a threshold value C_0 for a set of seven detunings Δ_{AC} . In accord with the expectation set by Fig. 4a, there is a decrease in the occurrence of large transit events for increasing Δ_{AC} in correspondence to the decrease in the effective atom–cavity coupling coefficient for large atom–cavity detunings. The full curves shown in Fig. 4b–d are the results of the theoretical calculation for these measurements, with the relevant cavity parameters (κ , h) determined from fits as in Fig. 2.

We first ask whether the data might be explained by an effective value g_0^e for the coherent coupling of atom and cavity field, without taking into account the fact that individual atoms transit at radial distances ρ that vary from atom to atom. Figure 4b examines this possibility for various values of g_0^e , assuming a coupling coefficient $g_0^e \psi_{A,B}(x) = g_0^e [\cos kx, \sin kx]$, averaged along one period in x (as in Fig. 4a). Apparently, an effective value $g_0^e/2\pi = 40$ MHz provides reasonable correspondence between theory and experiment for large events $C \geq 6$.

We adapt our theory to the actual situation of atoms arriving randomly at radial and circumferential coordinates by introducing a mesh grid over (ρ, x) , and then computing the cavity transmission function $T_F(t)$ from $\psi_{A,B}(\rho, x, z(t))$ for atomic trajectories $z(t)$ over this grid. We account for the time resolution $\delta t = 2 \mu\text{s}$ of our data acquisition by a suitable average of $T_F(t)$ over such time bins (as was also true in Fig. 4b). The results from these calculations are shown in Fig. 4c, d as the set of full curves for three values of coherent coupling g_0 for the cavity mode functions $\psi_{A,B}(\rho, x, z)$, where in Fig. 4b–d the theory is scaled to match the measured $N_{\text{drop}}^{\text{av}}(C \geq C_0)$ at $\Delta_{AC} = 0$. From such comparisons we determine a maximal accessible $g_0^m/2\pi$ of 50 ± 12 MHz. This conclusion is insensitive to the choice of cut-off C_0 over the range $4 \leq C_0 \leq 9$ for which we have significant transit events. Strong coupling with $g_0^m > (\kappa, \gamma)$ is thereby achieved, where $(\kappa, \gamma)/2\pi = (17.9 \pm 2.8, 2.6)$ MHz are the dissipative rates for the cavity field and the atom.

According to our calculations, $g_0^m/2\pi = 50$ MHz corresponds to the coupling rate expected at a distance of roughly 45 nm from the surface of the microtoroid. We estimate that due to the attractive van der Waals forces²⁷, atoms which enter the evanescent field with a distance $\rho \leq 45$ nm from the microtoroid are expected to strike its surface in less than $1 \mu\text{s}$, thus preventing such atoms from generating appreciable transit events in the transmission function T_F .

Thus, we report strong coupling for single atoms interacting with an optical resonator other than a conventional Fabry–Perot cavity. The monolithic microtoroidal resonators²² employed here have the capability of input–output coupling with small parasitic losses, with a demonstrated ideality of more than 99.97%²³. Moreover, quality factors $Q = 4 \times 10^8$ have been realized at $\lambda = 1,550$ nm (ref. 28) and

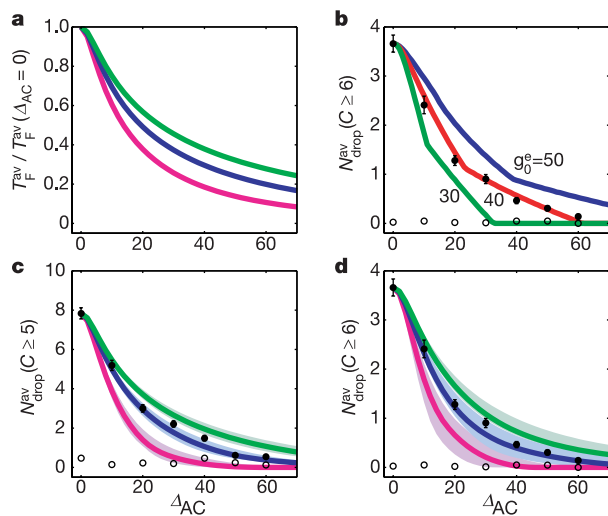


Figure 4 | Measurements of transit events as a function of the atom–cavity detuning Δ_{AC} . Events are shown in the presence of atoms (filled circles) and without atoms (empty circles), compared with the theoretical calculations (lines). **a**, Theoretical calculation for the average of the transmission $T_F(\omega_p = \omega_C)$ as a function of (Δ_{AC}, g_0) . Red, $g_0 = 35$; blue, $g_0 = 50$; green, $g_0 = 65$. **b–d**, Measurements of the average number of events per drop of the atom cloud $N_{\text{drop}}^{\text{av}}(C \geq C_0)$ plotted against the atom–cavity detuning Δ_{AC} , with $C_0 = 6$ (**b, d**) and $C_0 = 5$ (**c**). Error bars show ± 1 s.d. The data are taken for a cavity resonance equal to the probe frequency $\omega_C \approx \omega_p = \omega_A + \Delta_{AC}$. The full curves are theoretical results as discussed in the text. The widths of the curves are determined from the experimental uncertainties in (κ, h) . **b**, Theory for $N_{\text{drop}}^{\text{av}}(C \geq 6)$ without radial averaging to deduce an effective coupling $g_0^e/2\pi = 40$ MHz. Green, $g_0^e = 30$; red, $g_0^e = 40$; blue, $g_0^e = 50$. **c, d**, Theory for $N_{\text{drop}}^{\text{av}}(C \geq 5)$, $N_{\text{drop}}^{\text{av}}(C \geq 6)$, respectively, with radial and azimuthal averaging leading to $g_0^m/2\pi = 50$ MHz. Red, $g_0^m = 35$; blue, $g_0^m = 50$; green, $g_0^m = 65$.

$Q \approx 10^8$ at $\lambda = 850$ nm (ref. 26), with good prospects for improvements to $Q \approx 10^{10}$ (ref. 29). For these parameters, the efficiency for coupling single photons into and out of the resonator could approach $\varepsilon \sim 0.99$ – 0.999 (ref. 23), while still remaining firmly in the regime of strong coupling²⁶. Such high efficiency is critical for the realization of scalable quantum networks^{18,19} and photonic quantum computation²⁰. Indeed, of the diverse possibilities for the distribution and processing of quantum information with optical cavities^{5,7,8}, the system of single atoms coupled to microtoroidal resonators arguably provides one of the most promising avenues. Beyond efficient input–output coupling²³, strong coupling to a material system with long-lived internal states has now been showed, although here in a primitive, proof-of-principle setting. An outstanding technical challenge is to trap single atoms near the surface of the microtoroid, with one possibility having been investigated in ref. 30.

Received 2 June; accepted 1 August 2006.

- Miller, R. *et al.* Trapped atoms in cavity QED: coupling quantized light and matter. *J. Phys. B At. Mol. Opt. Phys.* **38**, S551–S565 (2005).
- Berman, P. (ed.) *Cavity Quantum Electrodynamics* (Academic, San Diego, 1994).
- Walther, H. Quantum optics of single atoms. *Fortschr. Phys.* **52**, 1154–1164 (2004).
- Raimond, J. M. *et al.* Probing a quantum field in a photon box. *J. Phys. B At. Mol. Opt. Phys.* **38**, S535–S550 (2005).
- Vahala, K. J. Optical microcavities. *Nature* **424**, 839–846 (2003).
- Nussmann, S. *et al.* Vacuum-stimulated cooling of single atoms in three dimensions. *Nature Phys.* **1**, 122–125 (2005).
- Khitrova, G., Gibbs, H. M., Kira, M., Koch, S. W. & Scherer, A. Vacuum Rabi splitting in semiconductors. *Nature Phys.* **2**, 81–90 (2006).
- Badolato, A. *et al.* Deterministic coupling of single quantum dots to single nanocavity nodes. *Science* **308**, 1158–1161 (2005).
- Wallraff, A. *et al.* Strong coupling of a single photon to a superconducting qubit using circuit quantum electrodynamics. *Nature* **431**, 162–167 (2004).
- Chiorescu, I. *et al.* Coherent dynamics of a flux qubit coupled to a harmonic oscillator. *Nature* **431**, 159–162 (2004).
- McKeever, J., Boca, A., Boozer, A. D., Buck, J. R. & Kimble, H. J. Experimental realization of a one-atom laser in the regime of strong coupling. *Nature* **425**, 268–271 (2003).
- McKeever, J. *et al.* Deterministic generation of single photons from one atom trapped in a cavity. *Science* **303**, 1992–1994 (2004).
- Keller, M., Lange, B., Hayasaka, K., Lange, W. & Walther, H. Continuous generation of single photons with controlled waveform in an ion-trap cavity system. *Nature* **431**, 1075–1078 (2004).
- Birnbaum, K. M. *et al.* Photon blockade in an optical cavity with one trapped atom. *Nature* **436**, 87–90 (2005).
- Legero, T., Wilk, T., Hennrich, M., Rempe, G. & Kuhn, A. Quantum beat of two single photons. *Phys. Rev. Lett.* **93**, 070503 (2004).
- Rempe, G., Thompson, R. J., Kimble, H. J. & Lalezari, R. Measurement of ultralow losses in an optical interferometer. *Opt. Lett.* **17**, 363–365 (1992).
- Hood, C. J., Ye, J. & Kimble, H. J. Characterization of high-finesse mirrors: loss, phase shifts, and mode structure in an optical cavity. *Phys. Rev. A* **64**, 033804 (2001).
- Cirac, J. I., Zoller, P., Kimble, H. J. & Mabuchi, H. Quantum state transfer and entanglement distribution among distant nodes in a quantum network. *Phys. Rev. Lett.* **78**, 3221–3224 (1997).
- Briegel, H.-J., van Enk, S. J., Cirac, J. I. & Zoller, P. in *The Physics of Quantum Information* (eds Bouwmeester, D., Ekert, A. & Zeilinger, A.) 192–197 (Springer, Berlin, 2000).
- Duan, L.-M. & Kimble, H. J. Scalable photonic quantum computation through cavity-assisted interactions. *Phys. Rev. Lett.* **92**, 127902 (2004).
- Treutlein, P. *et al.* Quantum information processing in optical lattices and magnetic microtraps. Preprint at (<http://arxiv.org/abs/quant-ph/0605163>) (2006).
- Armani, D. K., Kippenberg, T. J., Spillane, S. M. & Vahala, K. J. Ultra-high-Q toroid microcavity on a chip. *Nature* **421**, 925–928 (2003).
- Spillane, S. M., Kippenberg, T. J., Painter, O. J. & Vahala, K. J. Ideality in a fiber-taper-coupled microresonator system for application to cavity quantum electrodynamics. *Phys. Rev. Lett.* **91**, 043902 (2003).
- Braginsky, V. B., Gorodetsky, M. L. & Ilchenko, V. S. Quality-factor and nonlinear properties of optical whispering-gallery modes. *Phys. Lett. A* **137**, 393–397 (1989).
- Vernooy, D. W., Furusawa, A., Georgiades, N. Ph., Ilchenko, V. S. & Kimble, H. J. Cavity QED with high-Q whispering gallery modes. *Phys. Rev. A* **57**, R2293–R2296 (1998).
- Spillane, S. M. *et al.* Ultrahigh-Q toroidal microresonators for cavity quantum electrodynamics. *Phys. Rev. A* **71**, 013817 (2005).
- Courtois, J.-Y., Courty, J.-M. & Mertz, J. C. Internal dynamics of multilevel atoms near a vacuum-dielectric interface. *Phys. Rev. A* **53**, 1862–1878 (1996).
- Kippenberg, T. J., Spillane, S. M. & Vahala, K. J. Demonstration of ultra-high-Q small mode volume toroid microcavities on a chip. *Appl. Phys. Lett.* **85**, 6113–6115 (2004).
- Vernooy, D. W., Ilchenko, V. S., Mabuchi, H., Streed, E. W. & Kimble, H. J. High-Q measurements of fused-silica microspheres in the near infrared. *Opt. Lett.* **23**, 247–249 (1998).
- Vernooy, D. W. & Kimble, H. J. Quantum structure and dynamics for atom galleries. *Phys. Rev. A* **55**, 1239–1261 (1997).

Supplementary Information is linked to the online version of the paper at www.nature.com/nature.

Acknowledgements We thank M. Eichenfield, K. W. Goh and S. M. Spillane for their contributions to the early stages of this experiment, and T. Carmon, A. Gross and S. Walavalkar for their contributions to the current realization. The work of H.J.K. is supported by the National Science Foundation, the Disruptive Technology Office of the Department of National Intelligence, and Caltech. The work of K.J.V. is supported by DARPA, the Caltech Lee Center and the National Science Foundation. B.D., W.P.B. and T.J.K. acknowledge support as Fellows of the Center for the Physics of Information at Caltech. A.S.P. acknowledges support from the Marsden Fund of the Royal Society of New Zealand. E.W. acknowledges support as a Ford Predoctoral Fellow from the US National Academies.

Author Information Reprints and permissions information is available at www.nature.com/reprints. The authors declare no competing financial interests. Correspondence and requests for materials should be addressed to H.J.K. (hjkimble@caltech.edu).